*LAUTECH Journal of Engineering and Technology 19 (2) 2025: 239-250*

10.36108/laujet/5202.91.0252

# Application of Box-Behnken design for Optimizing the Production of Pyrolytic Bio-oil from Udara Seed in a Fixed-Bed Reactor

**[1]Ugwuodo C. B., [2]Itiri H. U., [3]Rose D.U, [4]Ezeocha L.C., and [5]Emmanuel I. N.**

[1,2,3,4]*Department of Chemical Engineering, College of Engineering and Engineering Technology, Michael Okpara University of Agriculture, Umudike.*

[5]*Department of Chemical Engineering, Nazarbayev University, Astana, Kazakstan*

**Article Info**

***Article history:***

**Received: Mar** 11, 2025
**Revised: May** 10, 2025
**Accepted: May** 19, 2025

***Keywords:***

Box-Behnken design (BBD), Bio-oil, Pyrolysis, Response surface methodology (RSM), Udara seed

***Corresponding Author:***

chijiokeugwuodo@mouau.edu.ng

*+234-8037156199*

**ABSTRACT**

***This work optimized the production of bio-oil from udara seeds using pyrolysis. Response surface methodology (RSM) was utilized to analyze the concurrent impact of temperature, particle size diameter, and inert gas flow rate on the percentage yield of bio-oil during the pyrolysis of udara seed. A three-variable, five-level Box-Behnken design (BBD) consisting of 17 experimental runs was employed to formulate a quadratic model for optimizing pyrolysis conditions. The optimum pyrolysis parameters for achieving the highest bio-oil production were a temperature of 422.9 °C, a particle size diameter of 2.5 mm, and an inert gas flow rate of 1.42 L/min. Under these conditions, the bio-oil yield was determined to be 59.73%. The model validation revealed no substantial discrepancy between anticipated and observed values. GC-MC analysis indicates that the predominant monounsaturated fatty acid made up 45.55% of the total fatty acid content, which depicts that the oil belongs to the linoleic acid group. The FTIR analysis reveals that the alkene group contributes to increased reactivity and combustion efficiency, boosts the octane number of the bio-oil, and decreases the boiling point of the oil. FTIR and GC-MS analysis findings confirm that the bio-oil was within ASTM specifications.***

## INTRODUCTION

Global energy consumption is significantly rising due to population increases and industrialization. Still, the world's fossil fuel supplies are finite and nearing depletion (Rajia *et al*., 2023). The usage of fossil fuels poses a significant threat to global climate change due to the high greenhouse gas emission rates generated from these fuels (Reshad *et al*., 2015). To achieve sustainable energy security, it is essential to establish a method that is energy-efficient, cost-effective, biodegradable, and utilizes renewable energy sources for fuel and chemical synthesis (Rajia *et al*., 2023). Biomass, the fourth most significant renewable energy source globally, accounts for 10–14% of the world's total energy reserves as a replacement for fossil fuels (Reshad *et al*., 2017). Biofuels derived from waste materials rely on biomass feedstock's abundant availability and suitability (Kumar *et al*., 2022). Non-edible oilseeds (vegetable oil), seed cake (derived from oil extraction), hulls (dehulled seeds), rice husks, sawdust, wheat stalks, sugarcane bagasse, algae, and various waste products are employed as raw materials for biofuel production (Reshad *et al*., 2017; Reshad *et al*., 2018; Reshad *et al*., 2019).

The utilization of agricultural waste, such as non-edible oilseed, for biodiesel production has been examined (Ahmed and Kishore, 2023; Reshad *et* *al*., 2018). The cake resulting from oil extraction from seeds is composed predominantly of lignocellulosic material (>90 mass%) rather than lipids (<5 mass%) (Reshad *et al*., 2018). It can generate commercially valuable organic chemicals and fuels through biochemical and thermochemical processes (Anas *et al*., 2024). The primary advantages of the pyrolysis process compared to other thermochemical methods (such as incineration, gasification, combustion, and carbonization) offers a lower operational temperature, no oxygen requirement, superior yield and quality of liquid products, and enhanced control over the reaction process (Reshad *et al*., 2018; Reshad *et al*., 2019). The pyrolysis process converts biomass into liquid, gas, and charcoal in an oxygen-free environment, typically at temperatures ranging from 300 to 700 °C (Rajia *et al*., 2023), with liquid pyro-oil yields from seeds varying between 30 and 70% (Abnisa and Wan-Daud, 2014). Pyrolysis yields three principal products: liquid bio-oil (condensable vapors), non-condensable gas, and solid charcoal (Aravind *et al*., 2023). The liquid bio-oil product has a fuel and non-fuel phase (Ahmed and Kishore, 2023). The non-fuel phase facilitates the recovery of essential compounds. In contrast, the other phase constitutes the desired fuel product, which may be isolated from the non-fuel phase using an appropriate solvent (Ahmed and Kishore, 2023; Aravind *et al*., 2023).

The African star apple, locally known as "Udara," and scientifically known as *Chrysophyllum albidum*, is a fruit indigenous to West Africa, including Nigeria. The tree is medium-sized, reaching 10–25 meters (Ehiagbonare *et al*., 2008). It produces round to oval fruits with a leathery orange to yellow skin. The pulp is sweet-sour and contains several flat, hard, bony, shiny, and dark brown seeds, encasing white-colored cotyledons (Ehiagbonare *et al*., 2008). The African star apple holds significant economic and cultural value in tropical Africa. Its fruits are consumed fresh and are rich in vitamin C and other nutrients. (Adebayo *et al*., 2012). Traditionally, various parts of the tree, including the bark and leaves, are utilized in herbal medicine to treat ailments such as diarrhea and skin infections (Omeje *et al*., 2019). It's often discarded seeds have gained attention as a potential feedstock for pyrolysis, a thermochemical decomposition process used to convert biomass into bio-oil, bio-char, and syngas (Sunday *et al*., 2024). Given its non-edible nature, the seed oil is an excellent feedstock for bio-oil production, circumventing the food-versus-fuel debate. Additionally, the oil can be used to produce soaps, cosmetics, and lubricants (Adebayo *et al*., 2012). Research indicates that defatted seed cakes of African star apples can be effectively utilized for bio-oil production through slow pyrolysis. In a study by Sokoto *et al*. (2020), defatted African star apple (ASA) seed cakes were pyrolyzed at temperatures ranging from 300 °C to 450 °C. The optimal bio-oil yield of 48.3% was achieved at 400 °C. The bio-oil composition was analyzed using Gas Chromatography-Mass Spectrometry (GC-MS), revealing major compounds such as acids (25.15%), phenolics (18.35%), and hydrocarbons (18.58%).

Abnisa *et al*. (2011) investigated the synthesis of liquid bio-oil from palm seed shells, achieving a maximum yield of 46.4 wt% at 500 ◦C utilizing a fixed-bed pyrolysis reactor. The pyrolysis of para-rubber seeds was examined by Chaiya and Reubroycharoen, revealing a maximum bio-oil yield of 38.22 wt% from the shell (2.18 mm particle size) and 34.35 wt% from the residue at 450 ◦C (Chaiya and Reubroycharoen, 2013). Reshad *et al*. (2015) conducted co-pyrolysis of rubber seed cake (RSC) and waste polystyrene (50 wt%: 50 wt%) to produce pyrolytic bio-oil, achieving a yield of 48.7 wt%. Ucar and Karagoz (2009) investigated the pyrolysis of pomegranate seed cake and documented a maximum liquid product yield of 54% at 500 ◦C. Bhattacharjee *et al*. (2021) investigated the conversion of rubber seed shells into activated carbon using steam activation.

To achieve optimal performance during pyrolysis, the independent variables must be tuned. The traditional optimization strategy involves the alteration of a single variable while maintaining the others at a constant level. This is frequently beneficial but fails to clarify the impact of the interaction among the numerous elements being examined (Sunday *et al*., 2024). The response surface methodology is an empirical statistical technique employed for multiple regression analysis of quantitative data obtained from statistically designed experiments by simultaneously resolving multivariate equations (Montgomery, 2005). The application of the design of experiments in response surface methodology facilitates the quantification of input levels for each variable and the targeted response level. The central composite, Box-Behnken, and Doehlert designs are widely utilized approaches in response surface methodology (González *et al*., 2021).

This study optimized the bio-oil production from udara seeds by pyrolysis. It examined the influence of temperature, particle size diameter, and inert gas flow rate on bio-oil yield. A mathematical correlation was developed using the Box-Behnken design of experiments to relate temperature, particle size diameter, and inert gas flow rate to maximize bio-oil yield.

## MATERIALS AND METHODS

### Materials and Equipment

The udara seeds were gathered from a farmland in Ndoro, Ikwuano, a local government area in Abia State, Nigeria. The equipment and apparatus used include a stainless-steel reactor, insulator (fibre glass), condenser, seal (iron gasket), fasteners (bolts and nuts), K-type temperature controller, $N_2$ gas cylinder, stopwatch, test sieves, weight balance, and electric heaters.

### Design of Experiment

A three-variable Box-Behnken design for response surface methods was utilized to examine the interactive impacts of temperature, particle size diameter, and inert gas flow rate on bio-oil yield at three levels (Table 1). The Box-Behnken design is suitable for examining quadratic response surfaces. It generates a second-degree polynomial model, which is then employed for process optimization with restricted experimental trials. This design requires a variable quantity of experimental trials as per equation (1).

$$N = k^2 + k + C_p \quad (1)$$

In this case, k signifies the factor number, which is 3. At the same time, Cp indicates the number of replications at the center point, which is 5. The design generated using Design Expert version 13 resulted in 17 trial runs, as shown in Table 2. The 17 experimental trials were randomized to enhance the effect of unaccounted variability in the observed responses due to external influences. The levels of the independent variables shown in Table 1 were established based on initial experiments. The range selection for the independent variables was guided by previous research (Okokpujie et al., 2023). The relationship between the encoded values and actual values is outlined in equation (2).

$$x_i = \frac{X_i - X_0}{\Delta X_i} \quad (2)$$

Where xi and Xi denote the encoded and actual values of the independent variable, respectively, Xo signifies the exact value of the independent variable at the midpoint. In contrast, ΔXi indicates the incremental variation of Xi. A second-degree polynomial was employed on the experimental data using Design Expert version 13 to estimate the dependent variable's response and predict the optimal point. The quadratic polynomial was expressed in equation (3).

$$Y = b_0 b_1 X_1 + b_2 X_2 + b_3 X_3 + b_{12} X_1 X_2 + b_{13} X_1 X_3 + b_{23} X_2 X_3 + b_{11} X_1^2 + b_{22} X_2^2 + b_{33} X_3^2 \quad (3)$$

In this model, Y represents the predicted response, while $X_1$, $X_2$, and $X_3$ denote the independent variables. The term $b_0$ serves as the offset, and $b_1$, $b_2$, and $b_3$ indicate the linear effects. Additionally, $b_{11}$, $b_{22}$, and $b_{13}$ are defined as the interaction terms.

Table 1. Coded and actual levels of the factors for the three-factor Box-Behnken design

| **Factor** | **Symbols** | **Coded and actual levels** | | |
|---|---|---|---|---|
| | | **- 1** | **0** | **+1** |
| **Temperature ($^0$C)** | $X_1$ | 400 | 500 | 600 |
| **Particle size (mm)** | $X_2$ | 1.00 | 3.00 | 6.00 |
| **Inert gas flow rate (L/min)** | $X_3$ | 1.00 | 1.25 | 1.50 |

**Pyrolysis Procedures**

The pyrolysis of udara seed was carried out in a lab-scale fixed-bed pyrolyzer. 50 g of dry udara seeds of varying particle sizes were introduced into the reactor for pyrolysis. The reactor was sealed with a lid and a steam gasket to ensure gas impermeability. Nitrogen gas was purged downstream of the tubular reactor at a flow rate of 1.5 L/min to establish an inert atmosphere. The heaters were heated to 600°C by adjusting the electrical control panel. A thermocouple was positioned at the reactor's apex to measure the internal temperature. The volatile products generated in the reactor were directed downward and subsequently passed through a condenser for cooling and collection. The condensation apparatus was established by immersing the filtering flask in cold water. The liquid oil and solid char were recovered separately, while non-condensable gas was vented into the atmosphere. The procedure was repeated for each experimental run. The bio-oil and char were weighed using a digital scale, documented, and securely stored in separate, well-sealed containers at room temperature. The yield percentage of pyrolysis products was calculated using Equation 4.

$$\%Yield\ of\ \ Product = \frac{mass\ of\ product}{mass\ of\ feedstock} \times 100 \quad (4)$$

**Characterization of bio-oil Fourier Transform infra-red (FTIR) Spectroscopy**

In this study, functional groups analysis of the bio-oil was carried out using Fourier transform infrared (FTIR) spectroscopy, Magna-IR550 (Nicolet, Madison). FTIR with an online pen plotter was used to produce the infrared (IR) spectra of the derived liquids. A small amount of the bio-oil was mounted on a potassium bromide (KBr) disc. The FTIR spectrum in the ranges of 500-3500cm$^{-1}$ was measured and recorded. The absorption frequency spectra were recorded and plotted. The standard IR- spectra of 61 organic compounds were used to identify the functional group of the components of the derived bio-oil (Rajia *et al*., 2023).

**GC-MS (Gas Chromatography-Mass Spectrometry)**

Gas chromatography-mass spectroscopy analysis was carried out on a Perkin Elmer Turbo Mass Spectrophotometer (Norwalk, CTO6859, and USA) incorporating a Perkin Elmer Auto sampler XLGC. The column utilized was a Perkin Elmer Elite -5 capillary column measuring 30m × 0.25mm with a film thickness of 0.25mm consisting of 95% Dimethylpolysiloxane. The carrier gas employed was helium at a flow rate of 0.5 mL/min. A sample injection volume of 1μl was employed. The inlet temperature was sustained at 250°C. The oven temperature was initially set to 110°C for 4 minutes, followed by a rise to 240°C. Subsequently, set to escalate to 280°C at a rate of 20°C, concluding with a duration of 5 minutes. The total duration was 90 minutes. The MS transfer line was sustained at a temperature of 200°C. The source temperature was sustained at 180°C. GCMS was analyzed using electron impact ionization at 70eV, and data was reviewed using total ion count (TIC) for compound identification and quantification. The spectra of the components were compared with the database of known component spectra recorded in the GC-MS library. Peak area measurements and data processing were conducted using Turbo-Mass OCPTVS-Demo SPL software.

## RESULTS AND DISCUSSION

### Statistical Analysis

The results from the 17 experimental trials conducted using the Box-Behnken design are displayed in Table 2. A second-order polynomial model was fitted to the data in Table 2 using multiple linear regression to identify the optimal pyrolysis conditions for maximizing bio-oil yield. The effects of temperature, particle size, and inert gas flow rate were quantitatively evaluated using reaction surface curves. Multiple regression analysis of the experimental data identified a second-degree polynomial that accurately characterizes the relationship between bio-oil yield and the variables mentioned above. The predicted bio-oil yield values derived from Equation (5) and experimental data are presented in Table 2.

$$Y = 47.86 - 3.95A - 1.82B - 2.10C + 5.05AB - 3.95AC + 1.40BC + 4.34A^2 + 0.1450B^2 + 7.55C^2 \quad (5)$$

The importance of the second-order polynomial fit for bio-oil yield was evaluated by analysis of variance (ANOVA), with results presented in Tables 3 and 4.

Table 2. Three-factor Box-Behnken design with experimental as well as predicted responses of the dependent variable

| Std | Run | Factor 1 A: Temperature C | Factor 2 B: Particle size mm | Factor 3 C: Inert gas flow rate L/min | Response1 Bio-oil yield | Predicted Bio-oil yield |
|---|---|---|---|---|---|---|
| **9** | 1 | 500 | 1.0 | 1.0 | 59.8 | 60.88 |
| **11** | 2 | 500 | 1.0 | 1.5 | 53.6 | 53.88 |
| **1** | 3 | 400 | 1.0 | 1.25 | 63.6 | 63.17 |
| **10** | 4 | 500 | 6.0 | 1.0 | 54.7 | 54.43 |
| **17** | 5 | 500 | 3.5 | 1.25 | 48.1 | 47.86 |
| **7** | 6 | 400 | 3.5 | 1.5 | 65.4 | 65.55 |
| **13** | 7 | 500 | 3.5 | 1.25 | 48.1 | 47.86 |
| **14** | 8 | 500 | 3.5 | 1.25 | 48.1 | 47.86 |
| **2** | 9 | 600 | 1.0 | 1.25 | 46.1 | 45.18 |
| **16** | 10 | 500 | 3.5 | 1.25 | 46.9 | 47.86 |
| **5** | 11 | 400 | 3.5 | 1.0 | 62.5 | 61.85 |
| **12** | 12 | 500 | 6.0 | 1.5 | 54.1 | 53.03 |
| **4** | 13 | 600 | 6.0 | 1.25 | 51.2 | 51.63 |
| **8** | 14 | 600 | 3.5 | 1.5 | 49.1 | 49.75 |
| **6** | 15 | 600 | 3.5 | 1.0 | 62 | 61.85 |
| **15** | 16 | 500 | 3.5 | 1.25 | 48.1 | 47.86 |
| **3** | 17 | 400 | 6.0 | 1.25 | 48.5 | 49.42 |

The model's coefficient of determination ($R^2$) was 0.9906 (Table 3), demonstrating that the model accurately represented the relationship between the analyzed variables. An $R^2$ score of 0.9906 signifies that the model explains 99.06% of the variability, with only 0.94% attributed to random chance. The coefficient of variation (C.V.) was calculated to be 1.81%. The Coefficient of Variation (C.V.)

indicates the precision of the executed processes. A low coefficient of variation indicates excellent reliability of the experiment (Montgomery, 2005). The adequate precision number (27.4067) quantifies the signal-to-noise ratio, with a ratio exceeding four (4) often considered favorable (Amenaghawon *et al*., 2013).

Table 3. Statistical information for ANOVA

| Source | Response value |
|---|---|
| **$R^2$** | 0.9906 |
| **Adjusted $R^2$** | 0.9786 |
| **Predicted $R^2$** | 0.8740 |
| **Std. Dev.** | 0.9693 |
| **C.V. %** | 1.81 |
| **Adeq Precision** | 27.4067 |

The results derived from the ANOVA analysis are reported in Table 4. Values of "Prob. > F" below 0.05 signify that the model terms are statistically significant. Values beyond 0.10 signify that the model terms lack significance. A model F-value of 82.35 and a negligible probability value [(Prob > F) less than 0.0001] indicate a significant model fit.

The regression model for bio-oil yield indicated that the terms A, B, C, $A^2$, and $C^2$ were significant at a 95% probability level. The terms AB, AC, and BC were significant, showing interactions among temperature and particle size diameter, temperature, and inert gas flow rate, particle size diameter, and inert gas flow rate. However, the interaction between the terms $B^2$ had no substantial impact on the yield of bio-oil generated during the pyrolysis of udara seed. The "Lack of Fit" F-value of 6.28 indicates an insignificant lack of fit. The "Lack of Fit" (Prob > F) score of 0.0540 indicates a 5.40% probability that the "Lack of Fit" F-value might arise from random variation.

Table 4. Analysis of variance (ANOVA) for a quadratic model of bio-oil yield.

| Source | Sum of Squares | df | Mean Square | F-value | p-value | Remark |
|---|---|---|---|---|---|---|
| **Model** | 696.39 | 9 | 77.38 | 82.35 | < 0.0001 | significant |
| **A-Temperature** | 124.82 | 1 | 124.82 | 132.85 | < 0.0001 | |
| **B-Particle size diameter** | 26.64 | 1 | 26.64 | 28.36 | 0.0011 | |
| **C-Inert gas flow rate** | 35.28 | 1 | 35.28 | 37.55 | 0.0005 | |
| **AB** | 102.01 | 1 | 102.01 | 108.57 | < 0.0001 | |
| **AC** | 62.41 | 1 | 62.41 | 66.42 | < 0.0001 | |
| **BC** | 7.84 | 1 | 7.84 | 8.34 | 0.0234 | |
| **$A^2$** | 79.49 | 1 | 79.49 | 84.60 | < 0.0001 | |
| **$B^2$** | 0.0885 | 1 | 0.0885 | 0.0942 | 0.7678 | |
| **$C^2$** | 239.69 | 1 | 239.69 | 255.11 | < 0.0001 | |
| **Residual** | 6.58 | 7 | 0.9396 | | | |
| **Lack of Fit** | 5.43 | 3 | 1.81 | 6.28 | 0.0540 | not significant |
| **Pure Error** | 1.15 | 4 | 0.2880 | | | |
| **Cor Total** | 702.97 | 16 | | | | |

**Optimization of Bio-oil yield**

Response surface plots were generated from the regression model to optimize the variables influencing bio-oil production from udara seed pyrolysis. The three-dimensional (3D) plots were generated by fixing one variable at the central point and varying the others within the experimental range. The response surfaces indicated the effects of temperature, particle size diameter, and inert gas flow rate on bio-oil production.

Figures 1 to 3 illustrate the three-dimensional and contour plots for optimizing bio-oil output. Figure 1 illustrates the three-dimensional and corresponding contour plots depicting bio-oil yield as a function of temperature and particle size diameter. An elevation in temperature and a corresponding rise in particle size diameter reduced bio-oil yield from approximately 49% to a minimum of 45% at a temperature of 600 °C and a particle size diameter of 1 mm. This aligns with the findings of González et al. (2021).

Figure 2 illustrates the impact of temperature and inert gas flow rate on bio-oil yield. The observed trend indicates a decrease in bio-oil yield up to 500 °C and 1.2 L/min for various combinations of increased temperature and inert gas flow rate; beyond this point, the bio-oil yield begins to rise, reaching approximately 65% at a temperature of 600 °C and an inert gas flow rate of 1.5 L/min. This aligns favorably with the findings of Bridgwater et al. (2019).

Figure 3 illustrates the impact of the interaction between particle size diameter and inert gas flow rate on bio-oil yield. An increase in particle diameter led to a negligible reduction in yield. Still, a similar rise in the inert gas flow rate caused a fall in bio-oil output, followed by an increase in yield at inert gas flow rates exceeding 1.2 L/min. This agrees with the report by Álvarez-Chávez et al. (201

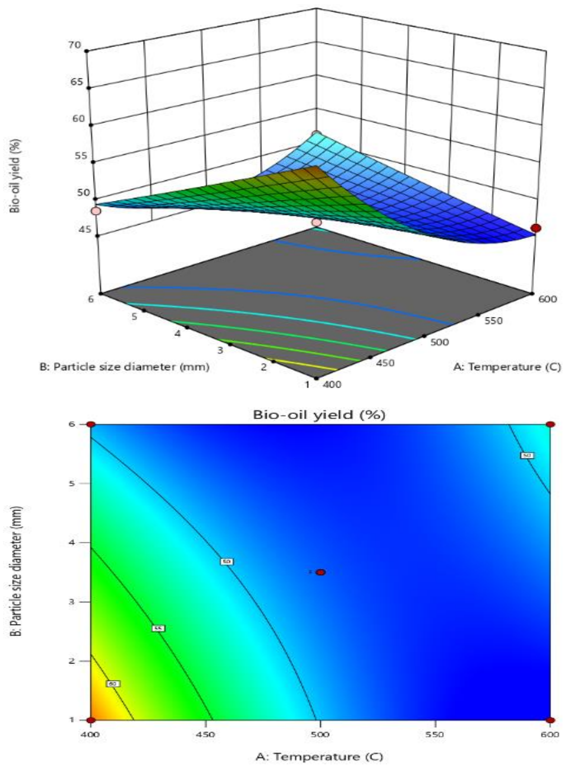


Figure 1. Response surface plot and the corresponding contour plot showing the effects of temperature and particle size diameter on bio-oil yield.

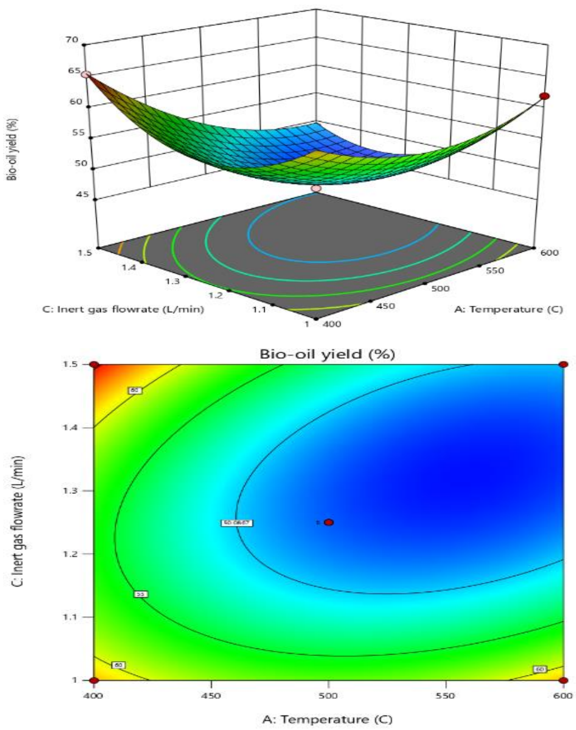

Figure 2. The response surface and contour plots show the effects of temperature and inert gas flow rate on bio-oil yield.

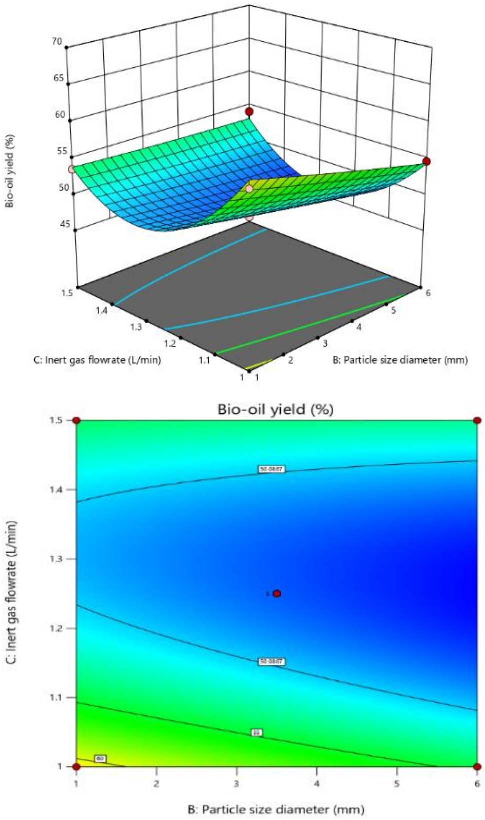


Figure 3. Response surface and contour plots showing particle size diameter and inert gas flow rate effects on bio-oil yield.

The model was analyzed to determine the optimal conditions and their corresponding levels. The model estimated a maximum bio-oil yield of 59.73%. The optimized pyrolysis parameters determined using RSM were 422.9 °C (temperature), 2.5 mm (particle diameter), and 1.42 L/min (inert gas flow rate). The elevated bio-oil levels seen at inert gas flow rates of 1.5 or 1.25 were not optimal, since these specific experimental runs failed to consider the optimized simultaneous influence of all three independent variables examined. The optimal inert gas flow rate of 1.42, derived from response surface methodology, represents the inert gas value at which the combined influence of all evaluated variables on bio-oil production was observed.

The inert gas flow rate is important in two respects. Firstly, creating an inert environment is required for pyrolysis to occur. Secondly, this nitrogen gas flow helps purge gaseous bio-oil into the condenser for condensation to occur and prevent secondary cracking of the vapourize bio-oil.

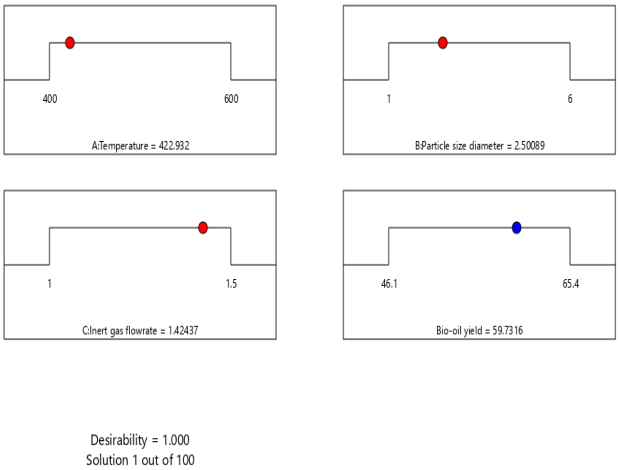


Figure 4. Numerical optimized value of the dependent and independent variables with desirability.

The validity of the findings forecast by the regression model was substantiated through the execution of numerous experiments under optimal pyrolysis circumstances (i.e., temperature: 422.9 °C, particle size diameter: 2.5 mm, and inert gas flow rate: 1.42 L/min). The results from three replications indicated that the average maximum bio-oil yield (58.94%) was around the projected value (59.73%). The strong correlation between the anticipated and measured values from these studies supports the validity of the response model.

**Results of Characterization of the Bio-Oil**

**FTIR analysis result of the bio-oil**

Fourier Transform Infrared (FTIR) Spectroscopy was used to identify the functional groups present in the bio-oil obtained from udara seed pyrolysis. The FTIR spectrum (Figure 5) displayed several prominent absorption bands, confirming the complex chemical nature of the pyrolytic oil.

A broad peak around 3347 $cm^{-1}$ was observed, characteristic of O–H stretching vibrations associated with hydroxyl groups. This suggests the presence of alcohols or phenolic compounds, common in lignocellulosic pyrolysis products. The broadness also implies hydrogen bonding, possibly due to residual moisture or water content, known to be prevalent in bio-oils.

Two sharp peaks at 2922 and 2855 $cm^{-1}$ were assigned to C–H stretching vibrations of aliphatic $–CH_2–$ and $–CH_3$ groups, indicating the presence of paraffinic hydrocarbons, likely originating from the thermal degradation of cellulose and hemicellulose.

A strong absorption at 1707 $cm^{-1}$ corresponded to C=O stretching vibrations, signifying the presence of carbonyl-containing compounds such as aldehydes, ketones, esters, or carboxylic acids. These compounds are typically formed during depolymerization of lignin and hemicellulose.

The peak at 1513 $cm^{-1}$ was attributed to aromatic C=C stretching or potentially asymmetric N=O stretching of nitro groups. In biomass pyrolysis, this region is often dominated by aromatic structures derived from lignin, indicating a significant phenolic content.

The region 1481–1377 $cm^{-1}$ exhibited several overlapping bands, indicative of C–H bending vibrations, suggesting the presence of branched and linear aliphatic hydrocarbons. Strong peaks observed between 1236 and 1096 $cm^{-1}$ were assigned to C–O stretching vibrations, commonly found in esters, alcohols, and ethers. These are typical decomposition products of lignin and hemicellulose.

Finally, the peak at 723 $cm^{-1}$ was attributed to $–CH_2$ rocking or aromatic C–H bending, indicative of long-chain alkanes or substituted benzene rings.

Overall, the FTIR spectrum confirms that the bio-oil contains a complex mixture of aliphatic, aromatic, hydroxyl, carbonyl, and ether/ester functional groups, consistent with the literature on lignocellulosic biomass pyrolysis products. These findings affirm the oxygen-rich and reactive nature of the bio-oil and its potential as a feedstock for bio-based chemicals or for upgrading into transportation fuels. These results align with the report of Ishaq *et al*. (2020).

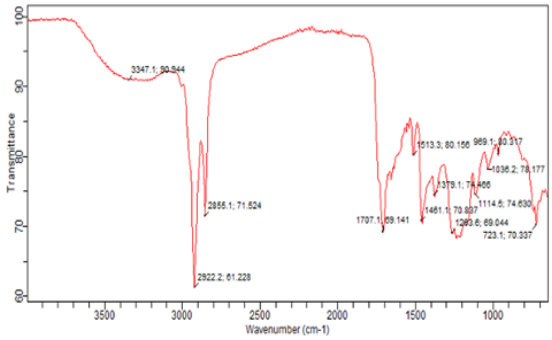


Figure 5. FT-IR spectrum of pyrolysis of udara seed for bio-oil

**Gas chromatography and mass spectrometry (GC-MS) analysis for the bio-oil.**

Gas Chromatography-Mass Spectrometry (GC-MS) analysis was performed to determine the fatty acid composition of the bio-oil sample derived from under seed. The chromatogram (Figure 6) revealed eight major fatty acids, spanning carbon chain lengths from C14 to C27, indicative of a complex mixture of saturated and unsaturated fatty acids.

The most abundant compounds were linoleic acid (45.55%) and palmitic acid (27.80%), representing unsaturated and saturated fatty acid classes, respectively. The detailed results are presented in Table 5.

The GC-MS results highlight a bio-oil composition that includes both saturated and unsaturated long-chain fatty acids, a trait typical of lipid-rich biomass feedstocks. The high proportion of linoleic acid (C18:2, 45.55%), an unsaturated fatty acid, suggests reactivity toward oxidation and potential instability upon storage. In contrast, the significant presence of palmitic acid (C16:0, 27.80%) and stearic acid (C18:0, 24.30%) contributes to oxidative stability and a higher cetane number, which is favorable for combustion in compression-ignition engines.

The detection of long-chain saturated fatty acids, such as arachidic (C20:0), behenic (C22:0), and cosnic acid (C27:0), is indicative of incomplete thermal degradation or high-molecular-weight lipid remnants, possibly from the partial breakdown of triglycerides or wax esters during pyrolysis. These compounds may contribute to higher viscosity, residual tar, or longer ignition delays if not adequately treated during downstream upgrading.

Overall, the distribution of fatty acids suggests that the bio-oil has potential as a precursor to biodiesel or as a feedstock for bio-based chemical synthesis. However, the high degree of unsaturation (particularly linoleic acid) may require antioxidant stabilization or hydrotreatment before storage or usage as a transportation fuel. This result compared well with the report of Okokpujie *et al*. (2023), Álvarez-Chávez *et al*. (2019), and Ude *et al*. (2023).

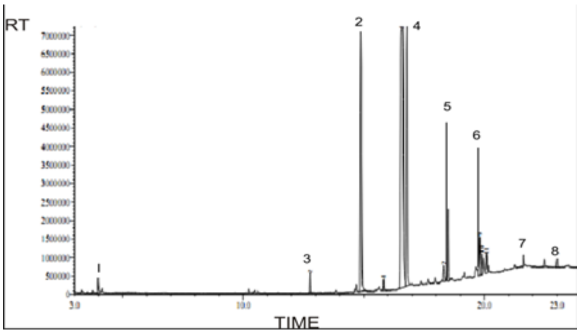


Figure 6. GC-MS of bio-oil compound produced from udara.

Table 5. Fatty Acid Composition of Bio-Oil Sample from Udara Seed via GC-MS

| S/No | Retention Time | Fatty Acid Present | Compound Names | Molecular Formula | % Concentration |
|---|---|---|---|---|---|
| **1.** | 12.75 | Tetradecanoic Acid | Myrisic Acid | $C_{14}H_{28}O_2$ | 0.90 |
| **2.** | 14.88 | Hexadecanoic Acid | Palmitic Acid | $C_{16}H_{32}O_2$ | 27.80 |
| **3.** | 15.80 | Heptadecanoic Acid | Margaric Acid | $C_{17}H_{34}O_2$ | 0.50 |
| **4.** | 16.60 | 9, Octadecadienoic Acid | Linoleic Acid | $C_{18}H_{31}O_2$ | 45.55 |
| **5.** | 16.80 | Octadecadienoic Acid | Stearic Acid | $C_{18}H_{34}O_2$ | 24.30 |
| **6.** | 18.80 | Eicosanoic Acid | Arachidic Acid | $C_{20}H_{40}O_2$ | 12.60 |
| **7.** | 20.10 | Docosanoic Acid | Behenic Acid | $C_{22}H_{44}O_2$ | 1.05 |
| **8.** | 21.60 | Heptacosanoic Acid | Cosnic Acid | $C_{27}H_{54}O_2$ | 0.65 |

## CONCLUSION

This study optimized the variables that could affect bio-oil production from the pyrolysis of udara seeds. These factors encompass temperature, particle size diameter, and inert gas flow rate. The investigation yields the following conclusions. The application of response surface methodology to identify the optimal conditions for bio-oil production from pyrolysis of udara seed has been established.

The pyrolysis of udara seeds is affected by temperature, particle size diameter, and inert gas flow rate. The bio-oil yield generated during pyrolysis is associated with temperature, particle size diameter, and inert gas flow rate, as determined by a validated quadratic regression model. The quadratic regression model accurately predicted the bio-oil yield generated during the pyrolysis of udara seed with high confidence. The optimal pyrolysis conditions included a temperature of 422.9 °C, a particle size diameter of 2.5 mm, and an inert gas flow rate of 1.42 L/min. Under these conditions, the maximum output of bio-oil was determined to be 59.73%.

Characterization of the bio-oil through GC-MS and FTIR analysis confirmed the presence of valuable compounds, including linoleic acid, palmitic acid, and esters, making it a potential feedstock for biofuel production.

## REFERENCES


Abnisa, F., Wan-Daud, W.M.A. (2014). A review on co-pyrolysis of biomass: An optional technique to obtain a high-grade pyrolysis oil. Energy Convers Manag 2014. https://doi.org/10.1016/j.enconman.2014.07.007 .

Abnisa, F., Wan Daud, W.M.A., Sahu, J. N. (2011). Optimization and characterization studies on bio-oil production from palm shell by pyrolysis using response surface methodology. Biomass Bioenergy 2011. https://doi.org/10.1016/j.biombioe.2011.05.011.

Adebayo, S. E., Orhevba, B. A., Adeoye, P. A., Musa, J. J., and Fase, O. J. (2012). Solvent extraction and characterization of oil from African star apple (C. albidum) seed. *Academic Research International*, 3(2), 178–183.

Ahmed, G., Kishore, N. (2023). Separation and extensive evaluation of properties of fuel and non-fuel portions of pyrolytic bio-oil obtained from Erythrina indica biomass. J Renew Sustain Energy 2023;15. https://doi.org/10.1063/5.0146201.

Amenaghawon, N. A., Nwaru, K. I., Aisien, F. A., Ogbeide, S. E., and Okieimen, C.O. (2013). Application of Box-Behnken Design for the Optimization of Citric Acid Production from Corn Starch Using Aspergillus niger. British Biotechnology Journal, 3(3): 236-245, 2013

Anas, A., Noorfidza, Y. H., Sharjeel, W., Ushtar, A., and Syed, A. G. (2024). Optimization of Operational Parameters Using Artificial Neural Network and Support Vector Machine for Bio-oil Extracted from Rice Husk. American Chemical Society ACS Omega XXXX, XXX, XXX−XXX. https://doi.org/10.1021/acsomega.4c03131

Aravind, S. V., Ahmed, G., Kishore, N. (2023). Pyrolysis of Delonix regia using metal oxide catalysts and solvent effect on fuel fraction of bio-oil. Results Eng 2023;17. https://doi.org/10.1016/j.rineng.2023.100876.

Álvarez-Chávez, B.J., Godbout, S., Le Roux, É., Palacios, J.H., Raghavan, V. (2019). Bio-oil yield and quality enhancement through fast pyrolysis and fractional condensation concepts. Biofuel Research Journal 24 1054-1064. DOI: 10.18331/BRJ2019.6.4.2

Bhattacharjee, A., Bhowmik, M., Paul, C., Das Chowdhury, B., Debnath, B. (2021). Rubber tree seed utilization for green energy, revenue generation, and sustainable development– A comprehensive review. Ind Crops Prod 2021;174. https://doi.org/10.1016/j.indcrop.2021.114186.

Bridgwater, A., and Peacocke, G. (2019). *Fast pyrolysis processes for biomass*. Renewable and sustainable energy reviews, 4(1), 1-73

Chaiya, C., Reubroycharoen, P. (2013). Production of bio-oil from para rubber seed using pyrolysis process. Energy Procedia 2013. https://doi.org/10.1016/j. egypro.2013.06.828.

Ehiagbonare, J. E., Onyibe, H. I., and Okoegwale, E. E. (2008). Studies on the isolation of *Chrysophyllum albidum* seed cotyledon and its potential as a food source. *African Journal of Biotechnology*, 7(20), 3629–3631.

González, M., Gómez, C., & López, J. (2021). Statistical optimization of extraction processes using Design Expert: A review. *Journal of Food Engineering*, 284, 110136.

Ishaq, M., Ullah, S., & Abbas, M. (2020). Valorization of agricultural residues: Biochar and bio-oil production from soursop seeds. *Waste Management*, 102, 116-124.

Kumar, A., Sharma, A., & Chandel, A. K. (2022). Recent advances in the economic and sustainable production of biofuels from lignocellulosic biomass. Bioresource Technology, 327, 124798. doi:10.1016/j.biortech.2021.124798.

Montgomery DC. (2005). Design and analysis of experiments, 6th ed. New York: John Wiley & Sons Inc; 2005.

Okokpujie, I. P., Anthony, O. O., Ejiroghene, O., Kunle, B., Emmanuel, S.A. A., Christian, O. O., Stephen, A. A., Esther T. A. (2023). Modeling and optimization of intermediate pyrolysis synthesis of bio-oil production from palm kernel shell. Cleaner Engineering and Technology 16 (2023) 100672

Omeje, K. O., Iroha, O. K., Edeke, A. A., Omeje, H. C., and Apeh, V. O. (2019). Characterization and fatty acid profile analysis of oil extracted from unexploited seed of African star apple (Udara). *OCL - Oilseeds and fats, Crops and Lipids*, 26, 10. https://doi.org/10.1051/ocl/2019007

Rajia, S., Uchhwas, B., Pranab, K. N., Muhammad, N. H., & Mohammad, I. (2023). Bio-oil production from rubber seed cake via pyrolysis: Process parameter optimization and physicochemical characterization. Energy Conversion and Management: X 20 (2023) 100429. https://doi.org/10.1016/j.ecmx.2023.100429.

Reshad, A. S., Tiwari, P., Goud, V. V. (2015). Extraction of oil from rubber seeds for biodiesel application: Optimization of parameters. Fuel 2015. https://doi.org/10.1016/j.fuel.2015.02.058.

Reshad, A. S., Tiwari, P., Goud, V. V. (2017). Thermal decomposition and kinetics of residual rubber seed cake and shell. J Therm Anal Calorim 2017. https://doi.org/10.1007/ s10973-017-6136-4.

Reshad, A. S., Tiwari, P., Goud, V. V. (2018). Thermo-chemical conversion of waste rubber seed shell to produce fuel and value-added chemicals. J Energy Inst 2018. https://doi.org/10.1016/j.joei.2017.09.002.

Reshad, A. S., Tiwari, P., Goud, V. V. (2019). Thermal and co-pyrolysis of rubber seed cake with waste polystyrene for bio-oil production. J Anal Appl Pyrolysis 2019. https://doi.org/10.1016/j.jaap.2019.03.010

Sokoto, M. A., Biswas, B., Kumar, J., & Bhaskar, T. (2020). "Slow pyrolysis of Defatted Seeds Cakes of African star apple and silk cotton for the production of bio-oil," Renewable Energy, Elsevier, vol. 146(C), pages 1710-1716.

Sunday, C. I., Michael, O. I., Olayomi, A. F., Atilade, A. O. (2024). Biogas production from Udara seeds inoculated with food waste digestate and its optimal output for energy utilities: Central composite design and machine learning approach. Energy Science & Engineering. Vol.12, Iss.9. Pg. 3614-3630 https://doi.org/10.1002/ese3.1748

Uçar, S., and Karagoz, S. (2009). The slow pyrolysis of pomegranate seeds: The effect of temperature on the product yields and bio-oil properties. J Anal Appl Pyrolysis 2009. https://doi.org/10.1016/j.jaap.2009.01.0

Ude, C. N., Christopher, N. I., Nwosu-Obiego, K., Patrick, C. N., Collins, N. O., Ndidi, F. A., Cordelia, N. E., & Uchenna, C. O. (2023). Optimization of dual transesterification of jatropha seed oil to lubricant using hybridized response surface methodology (RSM) and adaptive neuro-fuzzy inference system (ANFIS)-genetic algorithm (GA). Sustainable Chemistry for the Environment 4 100050. https://doi.org/10.1016/j.scenv.2023.100050